SURFICIAL GEOLOGY AND AGGREGATE POTENTIAL MAPPING IN NORTHEAST BRITISH COLUMBIA USING LIDAR IMAGERY

Tania E. Demchuk[1], Travis Ferbey[1], Ben J. Kerr[1] and Victor M. Levson[1]

ABSTRACT

Light detection and ranging (LiDAR) digital elevation models (DEMs) have proven to be an effective tool for mapping surficial features and aggregate potential in northeast British Columbia (BC). Northeast BC is characterized by low relief, and by subtle glacial landforms commonly masked by forest cover. For these reasons aerial photograph interpretation on its own is a somewhat ineffective aggregate exploration technique. The BC Ministry of Energy and Mines, in partnership with EnCana Corporation, is using LiDAR data with 10 m and 2 m horizontal resolution and vertical accuracies of up to 30 cm to map aggregate potential for portions of NTS map areas 94 I and P. To date, these data have helped in the identification and interpretation of glacial features and are responsible for numerous recent aggregate exploration successes in areas where there is a demand for construction aggregates. Some of these features are visible in lower resolution data sets such as airphotos and RADARSAT DEMs, while others are visible only in LiDAR DEMs. The latter is particularly true for low-relief features (*i.e.* 1 to 3 m high), which can be masked by vegetation in aerial photographs, and are often not resolved in RADARSAT DEMs. LiDAR DEMs have also proven to be a useful tool for detailed aggregate potential assessments of glaciofluvial features that are identifiable, but poorly defined, in other data sets.

T.E. Demchuk, T. Ferbey, B.J. Kerr and V.M. Levson, Surficial Geology and Aggregate Potential Mapping in Northeast British Columbia Using LiDAR Imagery in Summary of Activities 2005, *BC Ministry of Energy and Mines, pages 51-59.*

[1]Resource Development and Geoscience Branch, BC Ministry of Energy and Mines, PO Box 9323, Victoria, BC, V8W 9N3

Keywords: Quaternary geology, LiDAR, aggregate potential, northeast British Columbia, surficial geology, RADARSAT, surficial landforms, glacial features

INTRODUCTION

There is a requirement for more surficial geology and aggregate potential data in northeast British Columbia (BC). This demand is the result of the increased activity of the oil and gas industry in the region, and the need for construction aggregate for infrastructure development, upgrade, and maintenance. In 2002, the Oil and Gas Division of the British Columbia Ministry of Energy and Mines (BCMEM) initiated a Quaternary mapping program in northeast BC (Levson *et al.*, 2004; Ferbey *et al.*, 2005, this volume). The primary objective of this program is to identify new local sources of construction aggregate in areas where there is a demand.

Traditionally, surficial geology and aggregate potential mapping is carried out using aerial photograph interpretation. In northeast BC, however, this method on its own has proven to be somewhat ineffective due to the generally low topographic relief in the region, and the masking effect of vegetation on subtle surficial landforms. Other methods for aggregate potential mapping have therefore been employed, including the interpretation of seismic shot hole data, oil and gas logs, water well records, and geophysical surveys. This year, in partnership with EnCana Corporation, the Quaternary geology mapping group at BCMEM began to use light detection and ranging (LiDAR) data to map surficial geology for portions of NTS map areas 94 I and P. The objectives of using LiDAR data are to: (1) delineate surficial landforms and materials, particularly those associated with sands and gravels, and (2) interpret the Quaternary history of the region. This paper will address the first of these objectives.

STUDY AREA

Figure 1 outlines the study area (NTS map areas 94 I and P). The reader is directed to Levson *et al.* (2004) and Ferbey *et al.* (2005, this volume), for a more extensive discussion of the study area included in the northeast BC surficial geology and aggregate potential mapping program.

Northeast British Columbia is generally characterized by subdued topography and a blanket of clay-rich morainal and glaciolacustrine sediments. Glaciofluvial landforms, or landforms typically composed of sand and gravel, are rare in the region. The water table is near surface throughout much of the area, and black spruce (*Picea mariana*) bogs dominate. Locations even slightly elevated are typically vegetated by stands of trembling aspen (*Populus tremuloides*) and white spruce (*Picea glauca*).

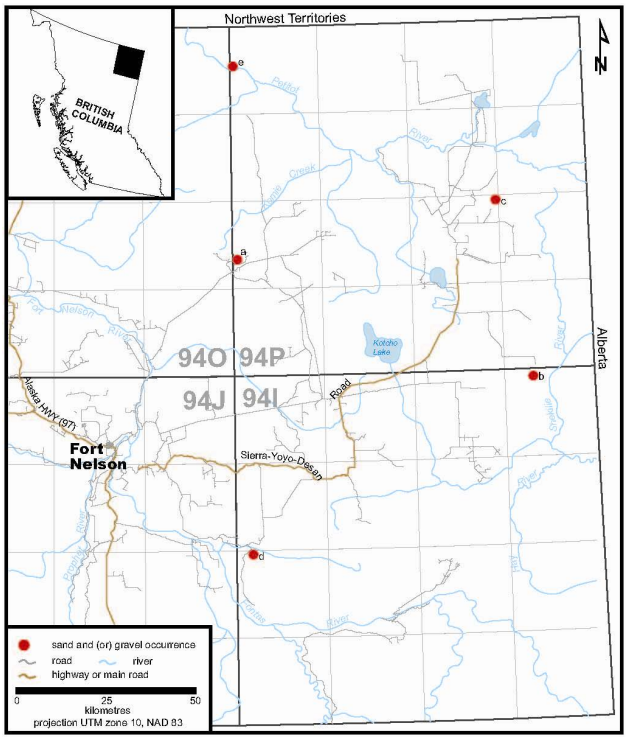

Figure 1. Study area and locations of selected aggregate occurrences.

LIGHT DETECTION AND RANGING TECHNOLOGY

Light detection and ranging (LiDAR) data are collected using an active sensor, mounted on the bottom of a fixed-wing aircraft or helicopter. LiDAR systems are based on principles similar to those of RADAR systems. Instead of using microwave frequency radiation (~10^{10} Hz), a swath of laser pulses, within the infrared frequency range (~10^{13} Hz) is fired at the ground at a user-specified rate. The transmitted laser pulses reflect off various surfaces and those reflections are recorded by a sensor on board the aircraft. The point spacing of the laser pulses (*i.e.* closeness of reflected pulses) is usually small (*e.g.* 1 point per 1.15 m^2 to 1.35 m^2), resulting in a high point density. This also differentiates LiDAR and satellite RADAR systems, as the latter typically record a lower point density. The LiDAR system also includes a differential GPS and an inertial measuring unit; these allow for exact positions of the aircraft, and x, y, z coordinates of point reflections, to be determined.

Light detection and ranging systems can be used to determine the range or distance to a target, for example the earth's surface. Known as range finders, these LiDAR sensors are able to detect multiple returns for a single laser pulse. In topographic mapping applications, the first return can be associated with the top of vegetation cover or tree canopy and the last with the ground surface. Because multiple returns can be detected, the resulting data is a series of x, y, and z coordinates that form a point cloud. This point cloud includes every point for which a reflection off a surface was recorded. Using a variety of software algorithms the top layer and bottom layer of points can be separated into two data files of x, y, and z coordinates. These two data files are typically associated with the first reflected and last reflected returns, respectively. From these two data files digital elevation models (DEMs) are created at user-specified resolutions that can highlight relative differences in elevation as little as 30 cm. Depending on how the data are interpolated two elevation models are typically produced: (1) full earth for generating a vegetation inclusive image, using the first returns detected by the sensor, and (2) bare earth for generating a vegetation exclusive image, using the last returns detected by the sensor. In areas with very dense vegetation cover the laser pulse may not penetrate to ground surface, making it more difficult to create an accurate bare earth DEM (Krabill *et al.*, 1984).

The accuracy of LiDAR data depends on various acquisition and post-processing parameters. Important acquisition parameters to consider are flight altitude, scanner frequency, inertial update rate (provide corrections for yaw, pitch, and roll of aircraft), point spacing, and base station range (Bufton *et al.*, 1991). Post processing of acquired data can involve a variety of software algorithms that interpolate the data clouds generated from the recorded laser pulse returns. Experience in data handling is important as the data smoothing that takes place during post processing can remove important features, or leave noise or unwanted information, in the final data set. A discussion of several algorithms used to remove early returns (*i.e.* vegetation) is provided by Haugerud and Harding (2001).

LIDAR IN OTHER QUATERNARY GEOLOGICAL APPLICATIONS

LiDAR data have been used in many Quaternary geological applications. For example, digital elevation models derived from LiDAR data are currently being used to investigate landslide history and help predict areas that may be susceptible to future slides (Carter *et al.*, 2001; Gold *et al.*, 2003; McKean and Roering, 2004; Schulz, 2004). Similar models are being used to map sinkhole development, which is often masked by vegetation and can pose serious hazards to existing and new infrastructure (Carter *et al.*, 2001). LiDAR data have also been used successfully to map Holocene faults around the Puget Lowland area of Washington State (Haugerud *et al.*, 2003; Sherrod *et al.*, 2003). In some cases these faults were previously unknown due to the masking effects of vegetation. LiDAR data are also being used in the Puget Lowland to update existing surficial geology and topographic mapping, as inaccuracies in previous mapping throughout this heavily forested area have been revealed by LiDAR imagery (Cox *et al.*, 2003; Easterbrook, 2003).

MAPPING SURFICIAL GEOLOGY USING LIDAR

The high point density of LiDAR data results in high vertical and horizontal accuracy, and is, therefore, very

useful for mapping surficial geology and glacial features. This high accuracy makes DEMs produced from these data effective for identifying small changes in elevation and, therefore, particularly useful in areas of low topographic relief such as northeast BC. LiDAR DEMs have proven to be a useful tool for mapping Quaternary landforms including kame-like deposits, fans, terraces, eskers, meltwater channels, and shorelines.

LiDAR DEMs are also useful for mapping details within a feature that are not seen in other data sets (*e.g.* lower resolution RADARSAT DEMS, DEMs produced by photogrammetry, and analog aerial photographs), because the bare earth model can remove the masking effects of vegetation. Cross-sections through selected features or areas, to aid in interpretation of genesis, can be produced in the digital environment because these data have x, y, and z values. These two attributes make LiDAR data particularly useful in areas of limited vertical relief.

Although a powerful data set on its own, LiDAR DEMs can be even more effective for mapping purposes when used in combination with other spatial data. For example, seismic shot hole data, geophysical well data (*e.g.* gamma logs), and orthophotos have also been used in conjunction with LiDAR DEMs to assess the aggregate potential of glacial features in the region.

The detail inherent to LiDAR DEMs can, however, show surface textures that do not represent surface topography. Areas with very dense ground vegetation, such as black spruce bogs, can make it difficult for the laser to penetrate through to bare ground surface. Mosses and other ground cover, and periglacial features such as peat palsas, can grow to create mounds and hummocks independent of the underlying topography. In some cases changes in elevation created by these vegetation surfaces can be up to 1 m (Figure 2a). The result is that textures in bare earth LiDAR imagery occasionally represent surfaces of dense vegetation. In places where the image displays this texture, digital orthophotos can be draped on top to investigate the genesis of these textures. In areas where this hummocky texture coincides with black spruce

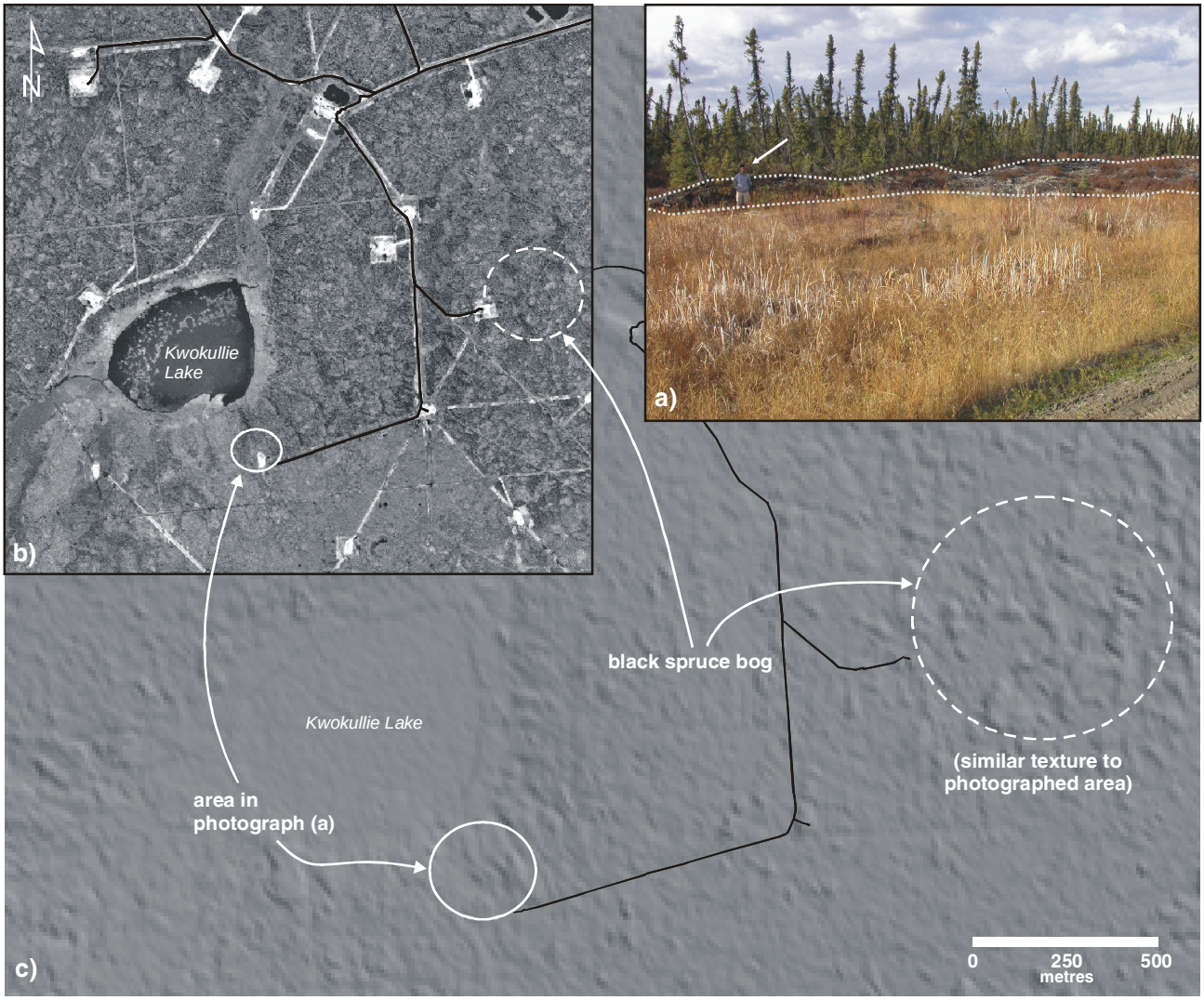

Figure 2. Dense vegetation mounds observed along Ish Road. (a) Thick vertical vegetation growth indicated by dashed line (person for scale, identified with arrow). (b) Black spruce bog is visible in aerial photographs and can coincide with the surface texture visible in LiDAR DEMs. (c) Vegetation related ground texture can be observed in bare earth DEMs (area circled coincides with bog area on aerial photograph). These textures are a result of the laser not being able to penetrate the dense, hummocky vegetation growth.

bog, it may represent changes in vegetation thickness not underlying topography (Figure 2b and c).

Acquisition of LiDAR data can be expensive (*e.g.* ~$250/km^2). However, the additional applications for LiDAR data in the oil and gas industry, such as locating dry well pad sites, siting pipeline routes, road alignments and seismic survey layouts, in addition to potential operational savings that can result from identifying new local sources of construction aggregate, could make investment in these data worthwhile.

AGGREGATE POTENTIAL MAPPING

LiDAR DEMs have been used successfully to map glacial features that are not seen in any other data sets. The following summary of features highlights some of the aggregate occurrences that have been found using LiDAR data. Figure 1 shows the locations of the features described below within the study area. References to field sites and data refer to shallow roadcuts, shovel excavations, and hand-auger holes, all 1 to 2 m below surface.

A series of sub-parallel southeast trending ridges, up to 8 m high, 75 m wide and 400 m long, occur near Komie Creek (Figure 1, location a), and are clearly visible in LiDAR DEMs (Figure 3a). A cross-section through the ridges shows typical heights and widths of about 5 m and 50 m, respectively. As determined by field investigations, the composition of these ridges is variable and they can contain fine to medium sands, pebble to cobble-sized gravels, and silty diamictons (Figure 3c and d). While these features are very well defined by LiDAR DEMs, the RADARSAT DEMs show only a vague outline of them. Several ridges are discernable in aerial photographs (Figure 4). However, where closely spaced, different ridges, or the breaks between them, are difficult to distinguish. As seen in Figure 4, vegetation nearly completely masks the detailed relief that is seen in LiDAR DEMs including the northwest limit of these

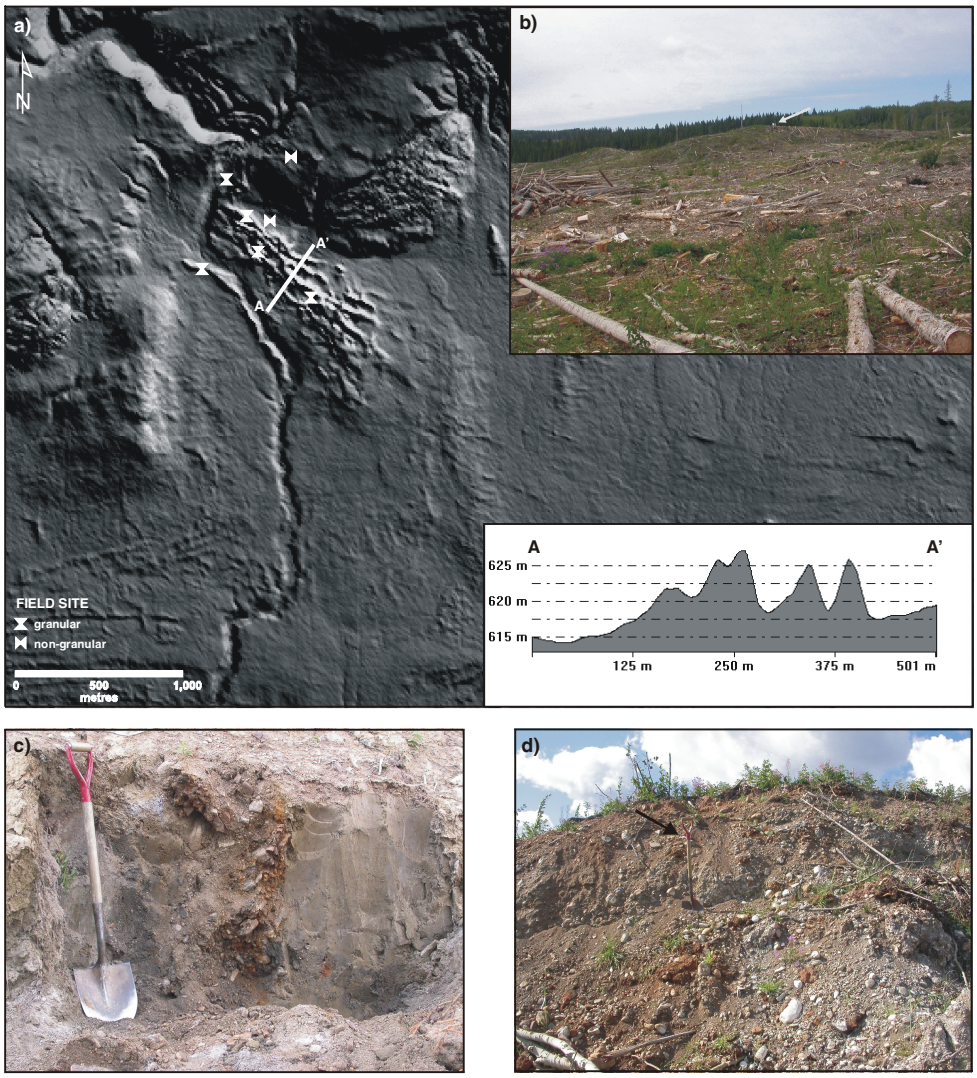

Figure 3. The Komie Creek gravel occurrence. (a) LiDAR DEM showing sub-parallel ridges composed of sands, gravels and diamictons. Inset cross-section (A to A') shows typical morphology and height of ridges, interpreted collectively as an esker complex. (b) An 8 to 10 m high ridge in cutblock (person for scale, identified with arrow). (c) The composition of a single ridge can be variable, as seen here with a silty diamicton in vertical contact with pebble to cobble-sized gravels and sands (1.2 m shovel for scale). (d) Exposure of sandy, cobble-sized gravels in roadcut through ridge (1.2 m shovel for scale, identified with arrow).

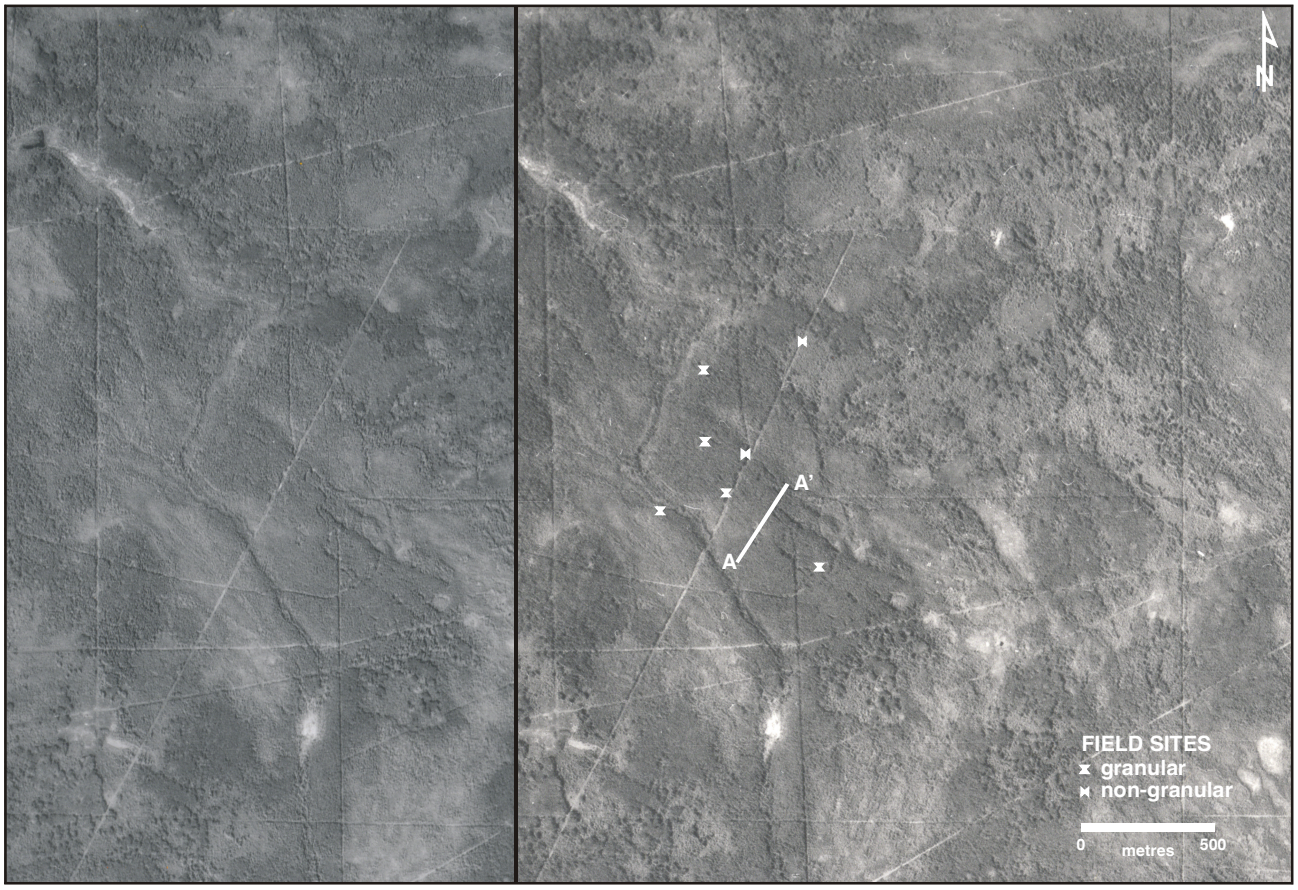

Figure 4. Aerial photograph stereogram of the Komie Creek gravel occurrence. Vegetation masks the detail of ridges within an esker complex that are clearly visible in a LiDAR DEM (*cf.* Figure 3a). Cross-section A to A', and field site locations, are the same as those provided in Figure 3a.

features. For example, in LiDAR DEMs this limit is clearly seen to be at a creek that drains south, while in aerial photographs the northwest portion of these features appears to grade into a forested slope. Interpreted as an esker complex, some of these ridges host an aggregate occurrence.

Sands and gravels near Shekilie River (Figure 1, location b) occur in two separate areas. Within Area 1 is an asymmetrical ridge-like feature that is elevated 10 m above surrounding topography, while within Area 2 occurs a series of curvilinear features that parallel slope and trend southwest (Figure 5). Sediments within Area 1 are composed mainly of well to very well rounded, pebble to cobble-sized quartzite gravels that have a medium sand matrix with a minor silty component. Northwest of the ridge, off the elevated area, a hand-auger excavation encountered silty sands. This feature may be a kame-like deposit.

Features within Area 2 are mainly composed of pebble to cobble-sized gravels that have a silt to silty-fine sand matrix. Exposed in a shallow shovel excavation, clasts are sub-angular to very well rounded and include abundant disc-shaped quartzites. Occurring at surface, these gravels likely overlie clays or silts as suggested by a hand-auger excavation directly to the south of, and elevationally below, the gravels (Figure 5). These curvilinear features are interpreted to be wave-washed shorelines of Glacial Lake Hay, which formed during the final retreat of the Laurentide ice-sheet from the region (Matthews, 1980). Alternatively, it is possible that these features are bedrock controlled and represent differential erosion, by ice, of the flat-lying shales and sandstones that underlie the region.

Another topographic high has been identified northeast of, and occurring at the same elevation as, Area 1 (Area 3, Figure 5). Within Area 3 is a feature that forms a flat-topped circular knob 10 m high and up to 425 m wide, and appears to be slightly drawn out to the west-northwest. The perimeter of the flat-topped area appears to be slightly elevated as the central portion of this feature is lower than the outer edge. Field assessment of this feature indicates that, at least at the top of the eastern perimeter, sandy silt diamicton occurs at surface. Area 3 has not been identified as an aggregate occurrence here. However, given that sands and gravels do occur in a morphologically similar feature 2 km to the southwest (*i.e.* Area 1), Area 3 does have potential to host granular material and warrants further field investigations.

LiDAR DEMs can also be effectively used to map glacial features that are visible in RADARSAT DEMs and aerial photographs. As LiDAR imagery can highlight details within features that may not otherwise be apparent. Two such examples are discussed below. Locations of these features are provided in Figure 1.

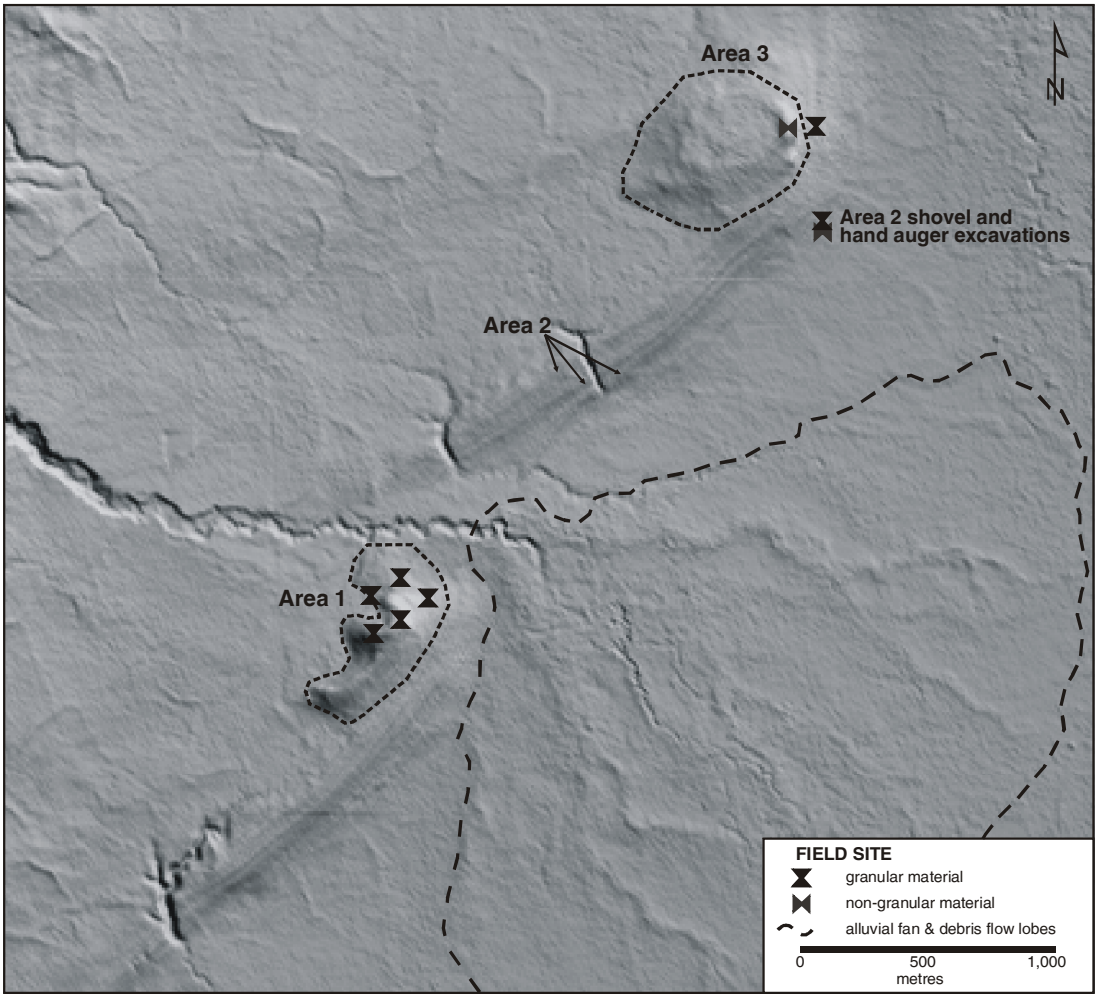

Figure 5. LiDAR DEM of Shekilie River area. Area 1 is a 10 m high kame-like feature that hosts sands and gravels at surface. Area 2 is a series of curvilinear features (indicated with arrows), interpreted to be wave-washed shorelines, that host pebble to cobble-sized gravels at surface. Within Area 3 is a feature similar to that identified in Area 1, that has been identified as having potential to host an aggregate occurrence. Also delineated here is a low gradient alluvial fan and debris flow lobes.

The East Kimea Creek gravel occurrence (Figure 1, location c) is a pronounced topographic high approximately 30 m high, 1000 m long, and 600 m wide. Surface observations and shallow shovel excavations indicate that cobble-sized gravels occur at surface. The kame-like feature is clearly visible in the RADARSAT DEM and in aerial photographs (Figure 6a and b, respectively). However, the LiDAR DEM provides a much more detailed image of the feature that not only enables more accurate mapping of it, but could also identify areas within it that may have better potential to host an aggregate occurrence (Figure 6c). Other kame-like deposits that are only visible in LiDAR DEMs have also been identified in other parts of the region, in some cases within one kilometre of an existing road; one such example is provided in Figure 7 (Figure 1, location d). This feature is up to 8 m high, 50 to 75 m wide and 225 m long (cross-sections A-A' and B-B', Figure 7), and appears to be part of a larger south-trending ridge system that may extend for 500 m or more. Exposed in a roadcut, the upper 150 cm of this feature is composed of 10 to 20 cm of silty diamicton that overlies 30 cm of silty pebble-sized gravels which in turn overlies >100 cm of silty-fine to coarse sand. The sandy unit appears to contain lenses of silty pebble-sized gravel similar to that of the overlying unit and, as the lower contact was not observed, is thought to extend below the 150 cm exposure. Other similarly sized features, composed of similar materials, occur in central and west-central 94P, also near existing roads. Features such as these, given their proximity to existing infrastructure, may provide useful local sources of sands and gravels for on-going road maintenance.

Using LiDAR DEMs, the aggregate potential of a large bench (5.25 km long and up to 1.5 km wide) along the Petitot River has also recently been assessed (Figure 1, location e). Field investigations on smaller terraces superimposed on the eastern end of the bench encountered sands and poorly sorted pebble to cobble-sized gravels at surface in tree throws and in shallow shovel excavations. Although this bench can be observed in both lower resolution RADARSAT DEMs, and in aerial photographs (Figure 8a and b, respectively), the LiDAR DEM clearly shows the details of the local geomorphology (Figure 8c). These higher resolution DEMs, in combination with field data, enable areas with higher aggregate potential to be identified. Many other features, that do not have

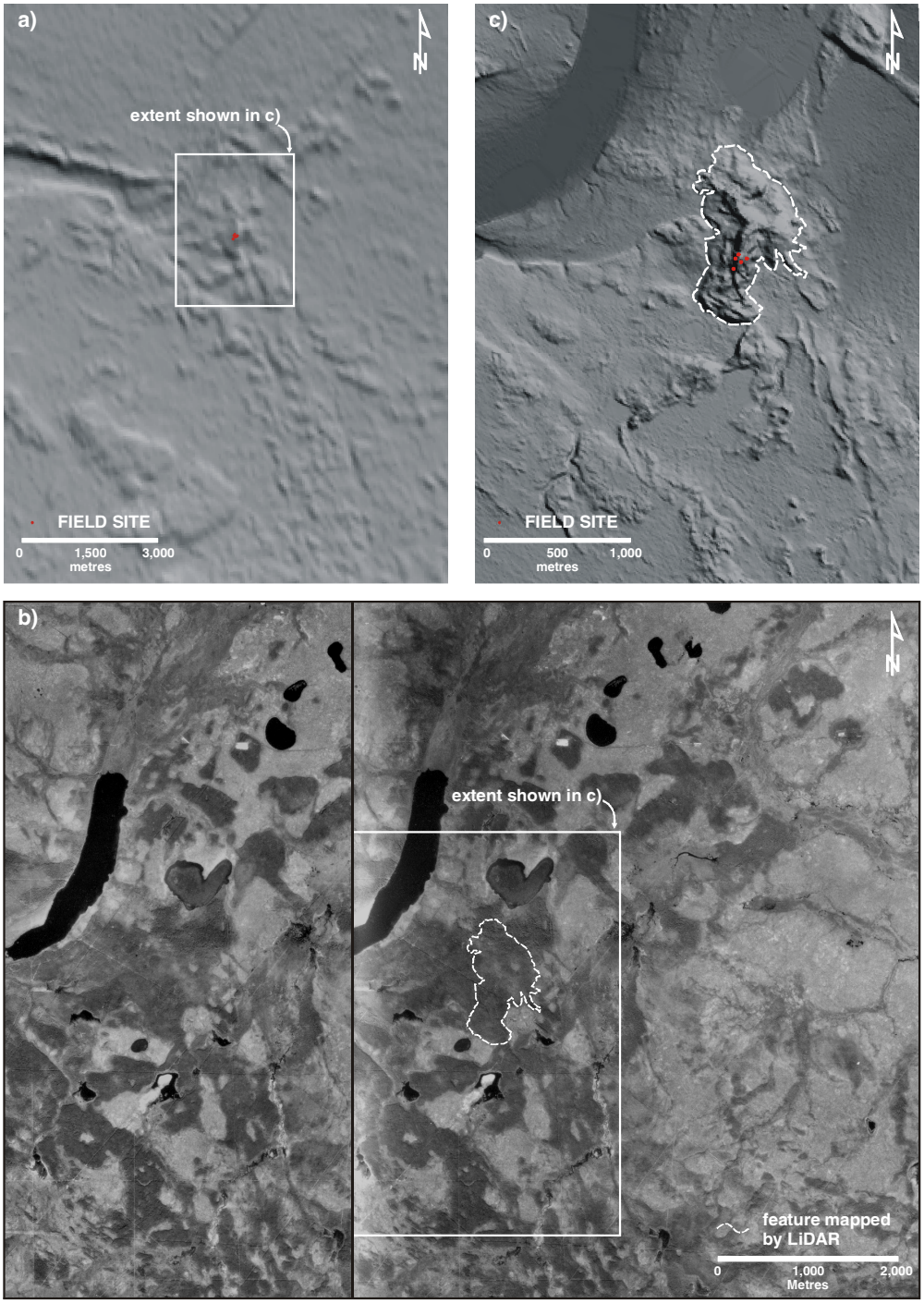

Figure 6. East Kimea Creek gravel occurrence. (a) This feature, which forms a prominent topographic high and is interpreted to be a kame deposit, is visible in the RADARSAT DEM (in vicinity of field sites) and (b) in aerial photographs. The polygon shown here was mapped using LiDAR data. As seen here, mapping using aerial photographs would produce a different polygon as the detail of the feature is masked by vegetation. (c) The LiDAR DEM provides more detailed information on the morphology of this feature and enables more accurate mapping of it and other related features that also have potential to host an aggregate occurrence.

aggregate potential, can also be seen Figure 8. For example, flutings trending southwest and moraines that generally parallel the Petitot River channel are also visible in the southeast portions of both the RADARSAT DEM and the aerial photograph (Figure 8a and b). In the LiDAR DEM, however, 1 to 2 m high asymmetrical ridges, inferred as ice-thrust features, can be seen on top of a morainal ridge south of Petitot River (Figure 8c, arrowed). Also more easily discernable in the LiDAR DEM are Holocene-age features such as point bars and terraces (visible along the length of Petitot River), meandering channels and oxbows (*e.g.* north of the bench), and gullies.

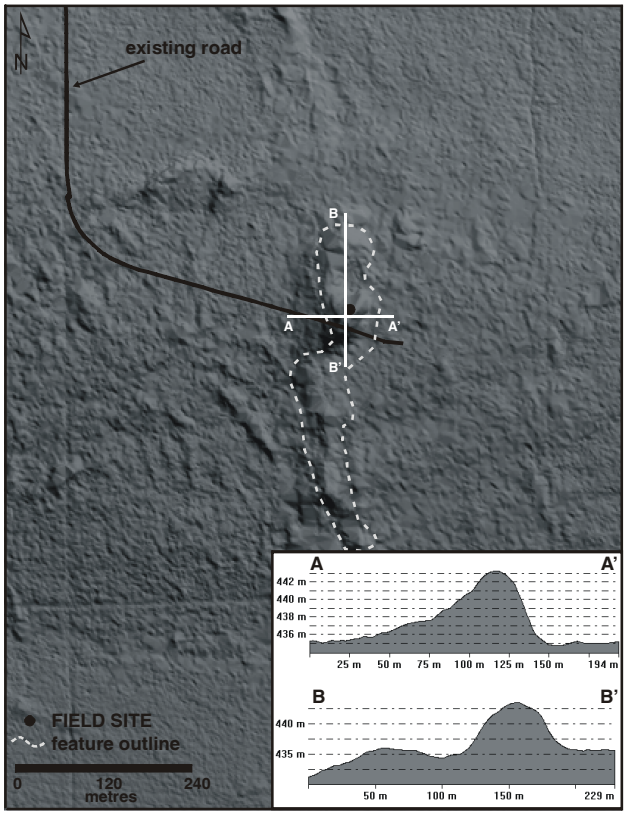

Figure 7. A small kame feature. Likely part of larger south-trending ridge system that extends for at least 500 m, this feature is mainly composed of sands and pebble-sized gravels. Small features like the one shown here can be found in the region, in some cases close to existing roads, making them useful as sources for construction aggregate.

SUMMARY

LiDAR DEMs have proven to be an effective tool for helping identify areas with good aggregate potential and are responsible for numerous recent aggregate exploration successes. Some of these occurrences are visible in other, lower resolution data sets such as aerial photographs and RADARSAT DEMs, while others are only visible in LiDAR DEMs. This is particularly true for aerially-smaller, low relief features. These features can often occur near existing infrastructure making them a useful local source of road-maintenance aggregate. LiDAR DEMs have also proven to be a useful tool for more detailed aggregate potential mapping of features that are identifiable, but poorly resolved, in other data sets. The accuracy and high resolution inherent to LiDAR data allow for the assessment of aggregate potential and calculation of preliminary volume estimates for a single feature, or specific area of it. Operational savings that may result from identification of aggregate resources using these data may make them a worthwhile investment for areas where there is a demand for local sources of sand and gravel.

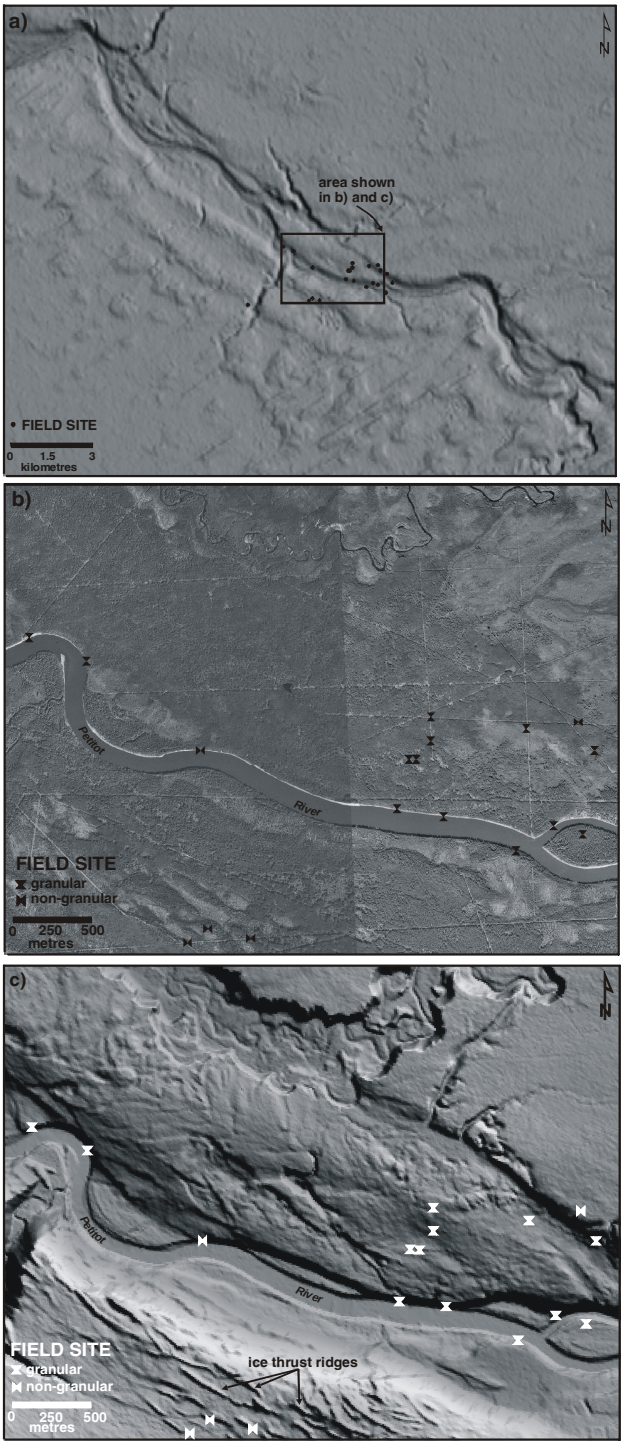

Figure 8. The Cabin Crossing gravel occurrence. This large bench along the Petitot River is visible in (a) RADARSAT DEMs, (b) aerial photographs, and (c) LiDAR DEMs. LiDAR imagery, however, is particularly effective at mapping the details of the feature (*e.g.* smaller terraces on the flanks of the large bench). Other geomorphic features visible in these figures are ice-thrust ridges superimposed on a morainal ridge (identified with arrows), large moraines and flutings, and Holocene-age point bars and terraces along Petitot River.

ACKNOWLEDGEMENTS

EnCana Corporation is thanked for the sharing of resources and data both in the office and field; LiDAR data are used here in partnership with EnCana Corporation. In particular the authors would like to thank Doug Anderson, John Neal, Tyson Pylypiw, Egil Ranestad, and Dennis Walberg. Jan Bednarski and Rod Smith of the Geological Survey of Canada, and Adrian Hickin and Michelle Trommelen of the British Columbia Ministry of Energy and Mines, are thanked for valuable discussions and insights into glacial features that occur in, and the Quaternary history of, the study area.

REFERENCES

Bufton, J.L., Garvin, J.B., Cavanaugh, J.F., Ramos-Izquierdo, L., Clem, T.D. and Krabill, W.B. (1990): Airborne laser profiling of surface topography; *Society of Photo-optical Instrumentation Engineers*, Volume 30, pages 72-78.

Carter, W., Shrestha, R., Tuell, G., Bloomquist, D. and Sartori, M. (2001): Airborne laser swath mapping shines new light on Earth's topography; *EOS, Transactions, American Geophysical Union*, Volume 82, no 46, pages 549-555.

Cox, B.F., Mahan, S.A. and Thoms, E. (2003): Geologic quadrangle mapping and studies of Quaternary stratigraphy in the Puget Lowland near Edmonds, Washington; *in* Abstracts with Programs, 2003 annual meeting, *Geological Society of America*, Volume 35, no 6, pages 80.

Easterbrook, D.J. (2003): Cordilleran Ice Sheet glaciation of the Puget Lowland and Columbia Plateau and alpine glaciation of the North Cascade Range, Washington; *in* Quaternary Geology of the United States, Easterbrook, D.J., Editor, *INQUA 2003 Field Guide Volume*, pages 265-286.

Ferbey, T., Hickin, A.S., Demchuk, T.E., and Levson, V.M. (2005): Northeast British Columbia Aggregate Mapping Program: a Summary of Selected Deposits and Occurrences Northeast of Fort Nelson; *in* Geological Fieldwork 2004, *British Columbia Ministry of Energy and Mines*, Paper 2005-1, pages 95-104.

Krabill, W.B., Collins, J.G., Link, C.E., Swift, R.N. and Butler, M.L. (1984): Airborne laser topographic mapping results; *American Society of Photogrammetry*, Volume 50, no 6, pages 685-694.

Gold, R.D., Wegmann, K.W., Palmer S.P., Carson R. J. and Spencer P.K. (2003): A comparative study of aerial photographs and LiDAR imagery for landslide detection in the Puget Lowland, Washington; *in* Abstracts with Programs, Cordilleran Section, 99th annual meeting, *Geological Society of America*, Volume 35, no 4, pages 12.

Haugerud, R.A., Harding D.J., Johnson S.Y., Harless, J.L. and Weaver, C.S. (2003): High-resolution LiDAR topography of the Puget Lowland, Washington – A bonanza for Earth Science; *GSA Today*, Volume 13, no 6, pages 4-10.

Haugerud, R.A. and Harding, D.J. (2001): Some algorithms for virtual deforestation (VDF) of LiDAR topographic survey data; *International Archives of Photogrammetry and Remote Sensing*, Volume 34, pages 211-217.

Levson, V.M., Ferbey, T., Kerr, B., Johnsen T., Bednarski, J., Smith, R., Blackwell, J. and Jonnes, S. (2004): Quaternary geology and aggregate mapping in northeast British Columbia: Applications for oil and gas exploration and development; *in* Geological Fieldwork 2004, *British Columbia Ministry of Energy and Mines*, Paper 2004-1, pages 29-40.

Link, L.E. and Collins, J.G. (1981): Airborne laser systems use in terrain mapping; *Fifteenth International Symposium on Remote Sensing of Environment, Ann Arbor, Michigan*, Volume 1, pages 95-110.

Matthews, W.H. (1980): Retreat of the last ice sheets in northeastern British Columbia and adjacent Alberta; *Geological Survey of Canada*, Bulletin 331, 22 pages.

McKean, J. and Roering, J. (2004): Objective landslide detection and surface morphology mapping using high-resolution airborne laser altimetry; *Geomorphology*, Volume 57, pages 331-351.

Schulz, W.H. (2004): Landslides mapped using LiDAR imagery, Seattle, Washington; *U.S. Geological Survey*, Open File Report 2004-1396, 11 pages.

Sherrod, B.L., Brocher, T.M., Weaver, C.S., Bucknam, R.C., Blakely, R.J., Kelsey, H.M., Nelson, A.R. and Haugerud, R.A, (2003): Evidence for a Late Holocene Earthquake on the Tacoma Fault, Puget Sound, Washington; *in* Abstracts with Programs, *Geological Society of America*, Volume 35, no 6, page 98.